Supplementary material for LHCb-PAPER-2019-001

We combine the results presented in this Letter with current knowledge of charm-mixing parameters to assess their impact on the world average. The combination procedure follows closely the methods of the Heavy Flavor Averaging Group. In addition to the results presented in this Letter, the following measurements are included in the combination:

- LHCb collaboration, R. Aaij *et al.*, *Updated determination of D^0–$\overline{D}^0$ mixing and CP violation parameters with $D^0 \to K^+\pi^-$ decays*, Phys. Rev. **D97** (2018) 031101, arXiv:1712.03220;
- Belle collaboration, B. R. Ko *et al.*, *Observation of D^0–$\overline{D}^0$ mixing in e^+e^- collisions*, Phys. Rev. Lett. **112** (2014) 111801, Erratum ibid. **112** (2014) 139903, arXiv:1401.3402;
- CDF collaboration, T. Aaltonen *et al.*, *Observation of D^0–$\overline{D}^0$ mixing using the CDF II detector*, Phys. Rev. Lett. **111** (2013) 231802, arXiv:1309.4078;
- BaBar collaboration, B. Aubert *et al.*, *Evidence for D^0–$\overline{D}^0$ mixing*, Phys. Rev. Lett. **98** (2007) 211802, arXiv:hep-ex/0703020;
- CLEO collaboration, D. M. Asner *et al.*, *Updated measurement of the strong phase in $D^0 \to K^+\pi^-$ decay using quantum correlations in $e^+e^- \to D^0\overline{D}^0$ at CLEO*, Phys. Rev. **D86** (2012) 112001, arXiv:1210.0939;
- LHCb collaboration, R. Aaij *et al.*, *Measurement of the charm-mixing parameter y_{CP}*, Phys. Rev. Lett. **122** (2019) 011802, arXiv:1810.06874;
- LHCb collaboration, R. Aaij *et al.*, *Measurement of the CP violation parameter A_Γ in $D^0 \to K^+K^-$ and $D^0 \to \pi^+\pi^-$ decays*, Phys. Rev. Lett. **118** (2017) 261803, arXiv:1702.06490;
- Belle collaboration, M. Starič *et al.*, *Measurement of D^0–$\overline{D}^0$ mixing and search for CP violation in $D^0 \to K^+K^-$, $\pi^+\pi^-$ decays with the full Belle data set*, Phys. Lett. **B753** (2016) 412 arXiv:1509.08266;
- LHCb collaboration, R. Aaij *et al.*, *Measurement of indirect CP asymmetries in $D^0 \to K^-K^+$ and $D^0 \to \pi^-\pi^+$ decays using semileptonic B decays*, JHEP **04** (2015) 043, arXiv:1501.06777;
- CDF collaboration, T. Aaltonen *et al.*, *Measurement of indirect CP-violating asymmetries in $D^0 \to K^+K^-$ and $D^0 \to \pi^+\pi^-$ decays at CDF*, Phys. Rev. **D90** (2014) 111103, arXiv:1410.5435;
- BaBar collaboration, J. P. Lees *et al.*, *Measurement of D^0–$\overline{D}^0$ mixing and CP violation in two-body D^0 decays*, Phys. Rev. **D87** (2013) 012004, arXiv:1209.3896;
- LHCb collaboration, R. Aaij *et al.*, *Measurement of mixing and CP violation parameters in two-body charm decays*, JHEP **04** (2012) 129, arXiv:1112.4698;
- LHCb collaboration, R. Aaij *et al.*, *Model-independent measurement of mixing parameters in $D^0 \to K^0_S\pi^+\pi^-$ decays*, JHEP **04** (2016) 033, arXiv:1510.01664;

Table 5: Updated global combinations of charm-mixing measurements.

Parameter	Value	Allowed interval		
		68.3% CL	95.5% CL	99.7% CL
x $[10^{-2}]$	0.38 ± 0.12	[0.26 , 0.50]	[0.14, 0.61]	[0.02, 0.71]
y $[10^{-2}]$	$0.655\,^{+0.062}_{-0.067}$	[0.588, 0.717]	[0.52, 0.78]	[0.44, 0.84]
$\lvert q/p \rvert$	$0.967\,^{+0.050}_{-0.045}$	[0.922, 1.017]	[0.88, 1.07]	[0.84, 1.13]
ϕ	$-0.070\,^{+0.079}_{-0.081}$	[−0.151, 0.009]	[−0.24, 0.09]	[−0.33, 0.19]

- Belle collaboration, T. Peng *et al.*, *Measurement of D^0–$\overline{D}^0$ mixing and search for indirect CP violation using $D^0 \to K^0_S\pi^+\pi^-$ decays*, Phys. Rev. **D89** (2014) 091103, arXiv:1404.2412;
- BaBar collaboration, P. del Amo Sanchez *et al.*, *Measurement of D^0–$\overline{D}^0$ mixing parameters using $D^0 \to K^0_S\pi^+\pi^-$ and $D^0 \to K^0_S K^+K^-$ decays*, Phys. Rev. Lett. **105** (2010) 081803, arXiv:1004.5053;
- Belle collaboration, A. Zupanc *et al.*, *Measurement of y_{CP} in D^0 meson decays to the $K^0_S K^+K^-$ final state*, Phys. Rev. **D80** (2009) 052006, arXiv:0905.4185;
- LHCb collaboration, R. Aaij *et al.*, *First observation of D^0–$\overline{D}^0$ oscillations in $D^0 \to K^+\pi^-\pi^+\pi^-$ decays and measurement of the associated coherence parameters*, Phys. Rev. Lett. **116** (2016) 241801, arXiv:1602.07224;
- BaBar collaboration, J. P. Lees *et al.*, *Measurement of the neutral D meson mixing parameters in a time-dependent amplitude analysis of the $D^0 \to \pi^+\pi^-\pi^0$ decay*, Phys. Rev. **D93** (2016) 112014, arXiv:1604.00857;
- BaBar collaboration, B. Aubert *et al.*, *Measurement of D^0–$\overline{D}^0$ mixing from a time-dependent amplitude analysis of $D^0 \to K^+\pi^-\pi^0$ decays*, Phys. Rev. Lett. **103** (2009) 211801, arXiv:0807.4544;
- Belle collaboration, U. Bitenc *et al.*, *Improved search for D^0–$\overline{D}^0$ mixing using semileptonic decays at Belle*, Phys. Rev. **D77** (2008) 112003, arXiv:0802.2952;
- BaBar collaboration, B. Aubert *et al.*, *Search for D^0–$\overline{D}^0$ mixing using doubly flavor tagged semileptonic decay modes*, Phys. Rev. **D76** (2007) 014018, arXiv:0705.0704.

The results are reported in Table 5 and Figure 5.

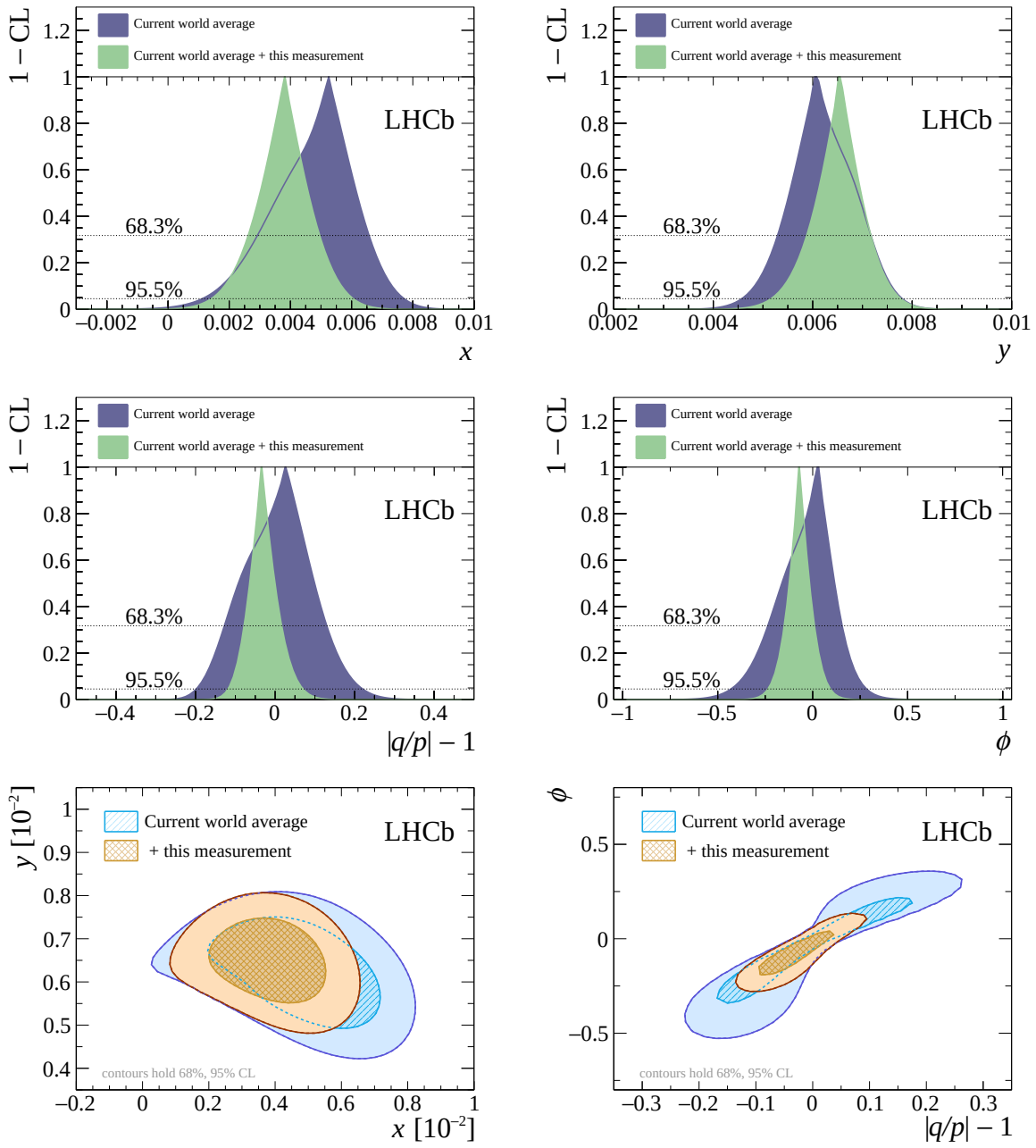

Figure 5: Impact of the results reported in this Letter on current global averages of charm-mixing parameters. The hatched and shaded areas in the bottom panels indicate the 68% and 95% confidence regions, respectively.

Table 6: Summary of the uncertainties in units of 10^{-3}. Numbers outside parentheses refer to the combined fit to prompt and semileptonic data, those inside the first (second) parentheses refer to the fit to the prompt-only (semileptonic-only) data. The total systematic uncertainty is the sum in quadrature of the individual components. The uncertainties due to the CLEO inputs are included in the statistical uncertainty. We also report separately the contributions due to the CLEO inputs and to our sample size to ease comparison with other sources.

Source	x_{CP}	y_{CP}	Δx	Δy
Secondary charm decays	0.24 (0.44) (0.00)	0.36 (0.65) (0.00)	< 0.01	< 0.01
Unrelated $D^0\mu^-$ combinations	0.34 (0.00) (0.94)	0.31 (0.00) (0.60)	< 0.01	< 0.01
Reconstruction and selection biases	0.08 (0.24) (0.08)	0.94 (1.37) (0.21)	0.22 (0.24) (0.28)	0.25 (0.29) (0.22)
Mass-fit model	0.04 (0.02) (0.10)	0.03 (0.08) (0.15)	< 0.01	0.03 (0.04) (< 0.01)
VELO length scale	< 0.01	< 0.01	< 0.01	< 0.01
Input D^0 lifetime	< 0.01	< 0.01	< 0.01	< 0.01
Total systematic	0.43 (0.50) (0.95)	1.05 (1.52) (0.65)	0.22 (0.24) (0.28)	0.25 (0.29) (0.22)
CLEO inputs	0.70 (0.65) (0.87)	1.22 (1.54) (1.35)	0.19 (0.25) (0.28)	0.26 (0.36) (0.65)
Statistical (w/o CLEO inputs)	1.46 (1.76) (2.64)	3.35 (4.02) (6.12)	0.68 (0.74) (1.67)	1.58 (1.76) (3.93)
Statistical	1.62 (1.87) (2.78)	3.57 (4.30) (6.27)	0.70 (0.78) (1.69)	1.60 (1.80) (3.98)

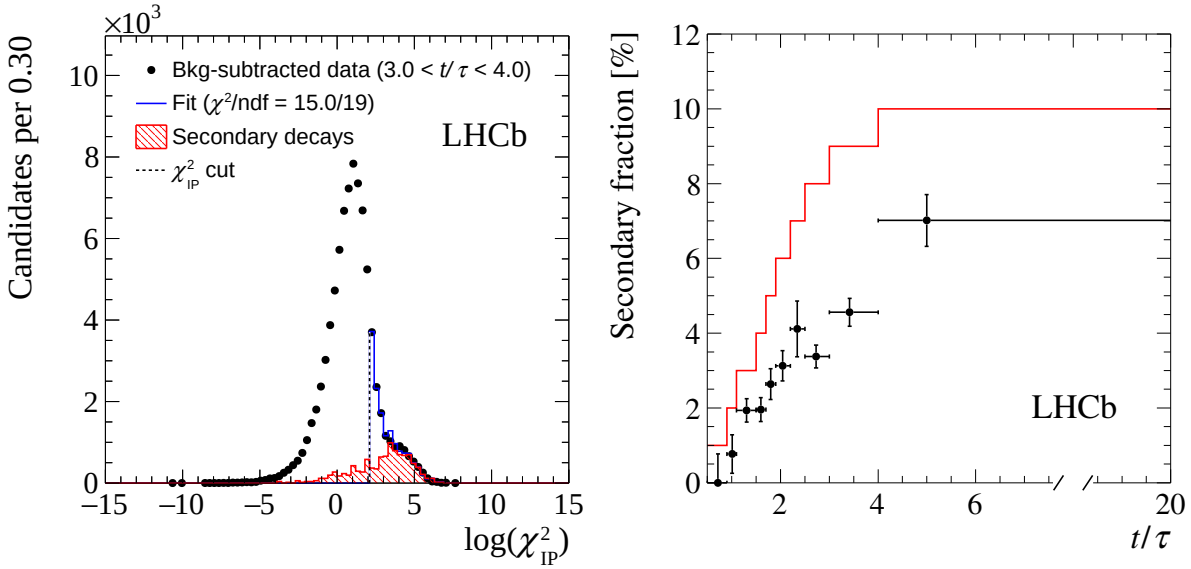

Figure 6: (Left) Example fit to the distribution of the D^0 $\log(\chi^2_{\rm IP})$ of background-subtracted $D^{*+} \to D^0(\to K^0_S\pi^+\pi^-)\pi^+$ candidates selected by an inclusive D^{*+} trigger; the distribution for the secondary decays is determined from prompt candidates that are also reconstructed as $\overline{B} \to D^{*+}\mu^- X$ decays. (Right) Observed fraction of secondary D^{*+} decays as a function of decay time, for candidates selected by the inclusive D^{*+} trigger; in the evaluation of the systematic uncertainties, the larger secondary fraction indicated by the red line is considered to account for uncertainties in the extrapolation of the contamination fraction to the full sample.

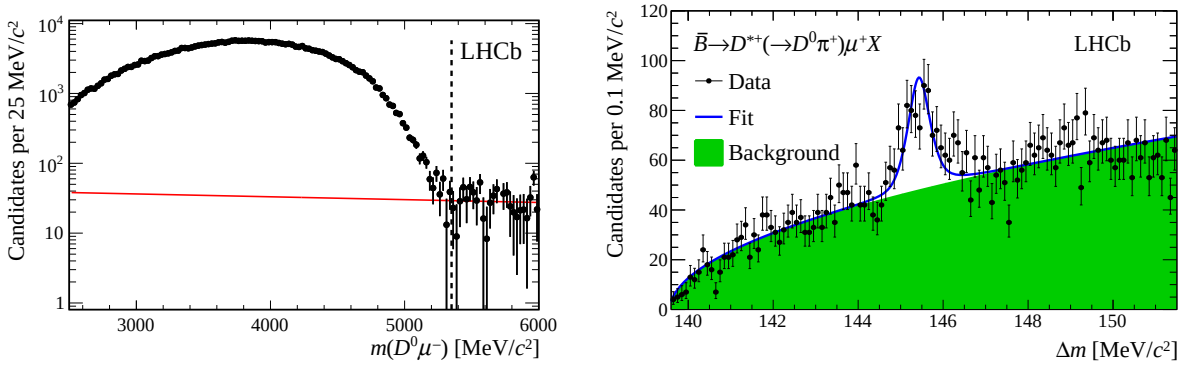

Figure 7: (Left) Example distribution of the visible $\overline{B}$ mass for $\overline{B} \to D^0(\to K^0_S\pi^+\pi^-)\mu^- X$ candidates. The unphysical region on the right of the dashed line is fitted with an exponential function (red) to extract the fraction of random $D^0\mu^-$ combinations in the signal region. The background in D^0 mass is statistically subtracted. (Right) Example fit to the Δm distribution of $\overline{B} \to D^{*+}(\to D^0\pi^+)\mu^+ X$ candidates where the muon and soft-pion charges have the same sign. The fraction of these candidates is a measure of the fraction of random $D^0\mu^-$ combinations.

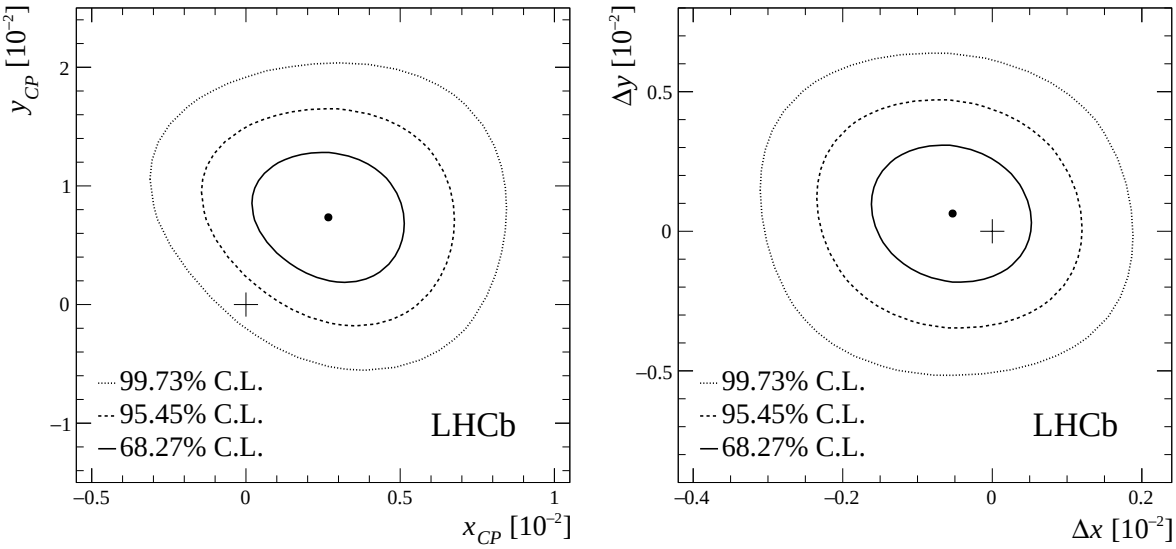

Figure 8: Two-dimensional 68.3%, 95.5%, and 99.7% confidence-level (CL) contours in the (left) (x_{CP}, y_{CP}) and (right) $(\Delta x, \Delta y)$ planes, as determined from the fit to the combined prompt and semileptonic data. The no-mixing hypothesis (indicated by the cross in the left plot) has a p value of 1% and the no-CP-violation hypothesis (indicated by the cross in the right plot) has a p value of 72%.

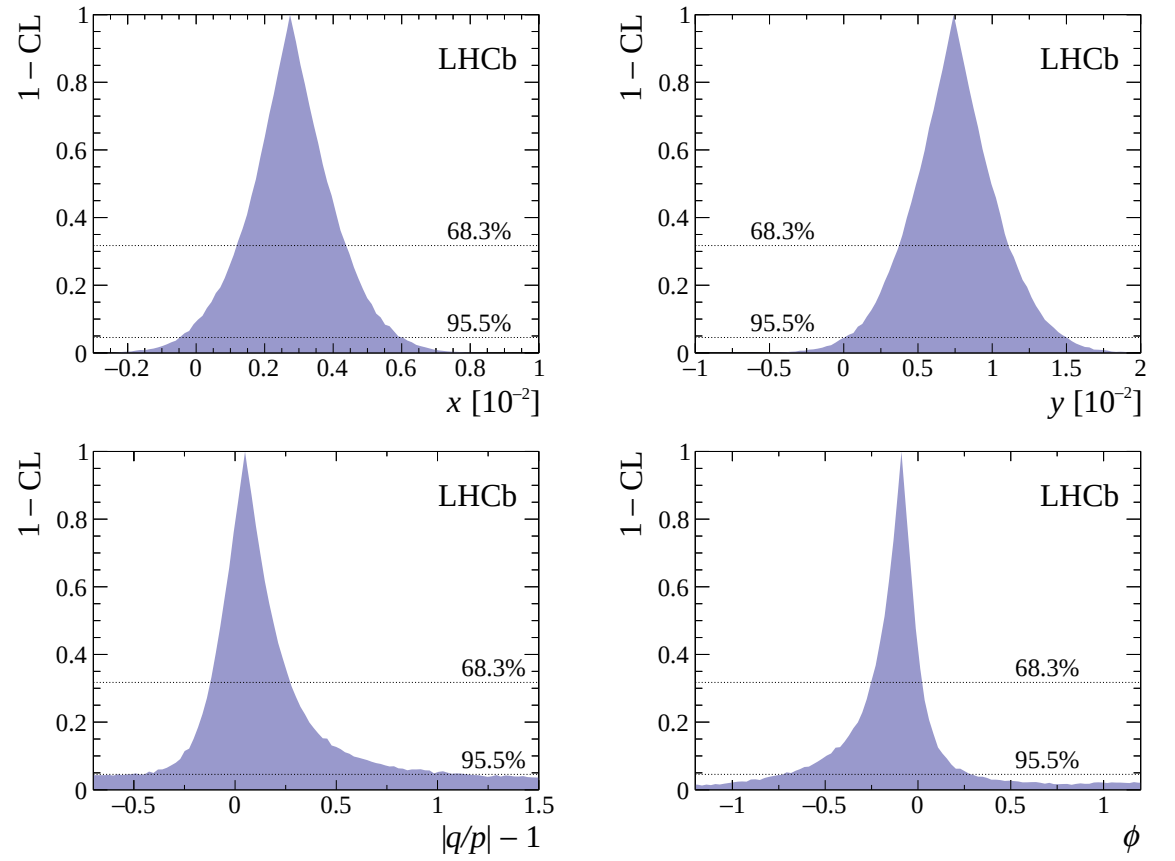

Figure 9: Distribution of 1 − CL for the derived parameters x, y, $|q/p|$, ϕ.

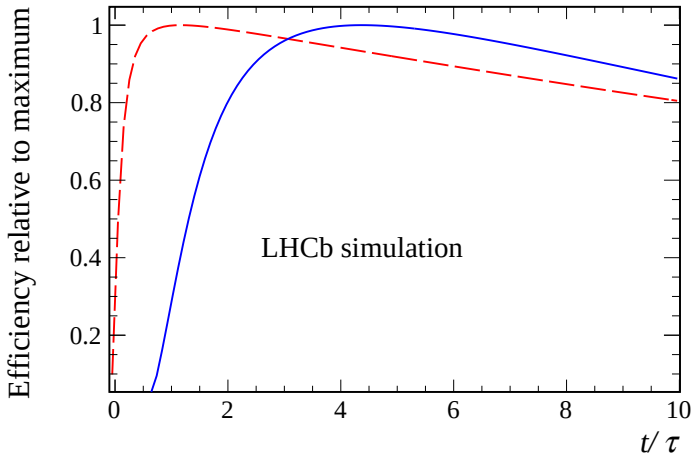

Figure 10: Efficiency (normalized to unity at its maximum) as a function of decay time as determined from simulation for the (solid blue) prompt and (dashed red) semileptonic samples. The samples reconstructed with long and downstream K^0_S candidates have been combined.

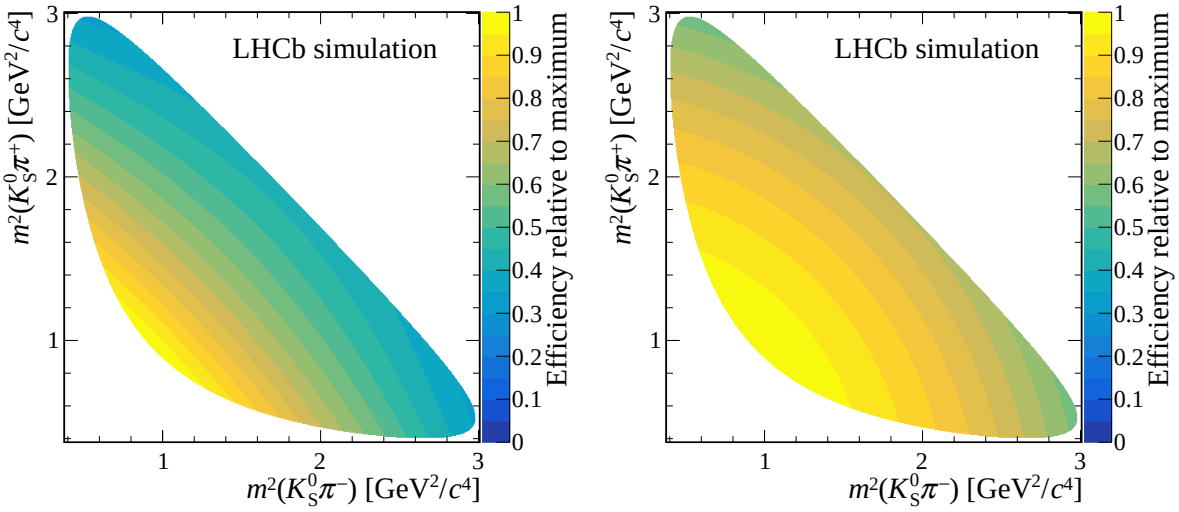

Figure 11: Efficiency as a function of the Dalitz-plot position, as determined from simulation for the (left) prompt and (right) semileptonic samples. The samples reconstructed with long and downstream K^0_S candidates have been combined.

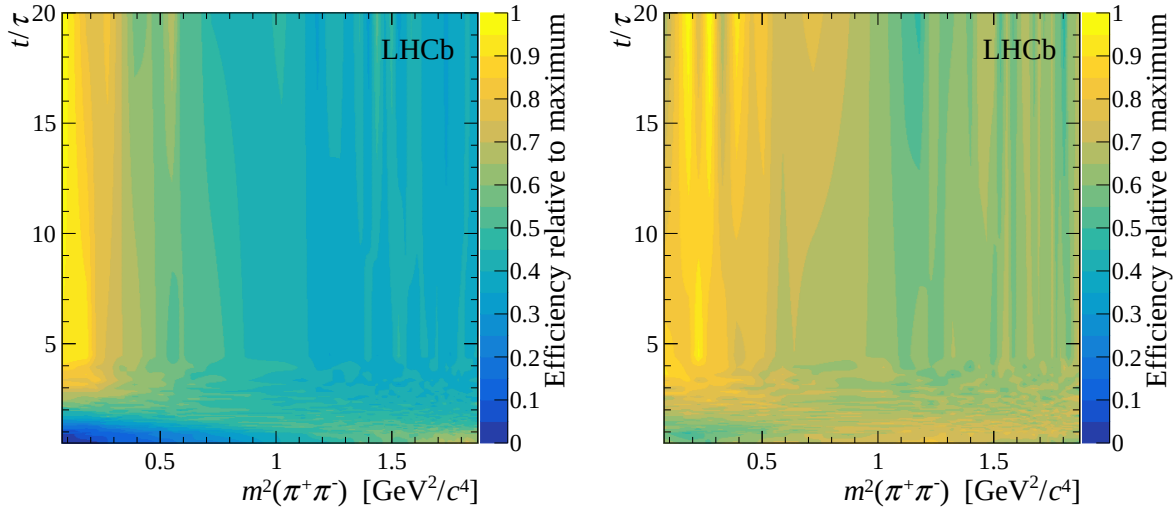

Figure 12: Smoothed distribution of the efficiency as a function of decay time and $m^2(\pi^+\pi^-)$ in $D^{*+} \to D^0(\to K^0_S\pi^+\pi^-)\pi^+$ decays, as determined from the data with (left) downstream and (right) long K^0_S candidates.

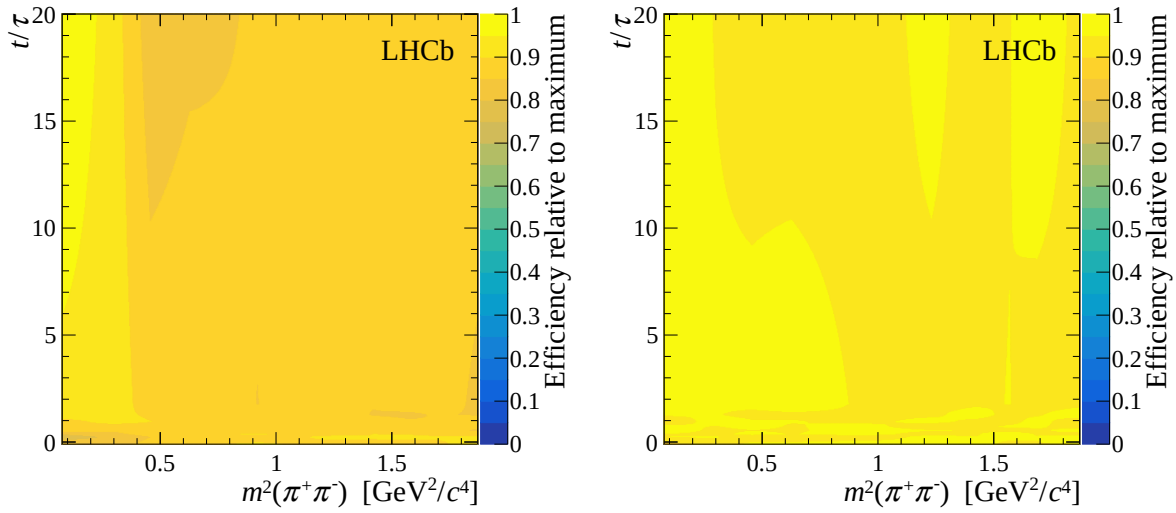

Figure 13: Smoothed distribution of the efficiency as a function of decay time and $m^2(\pi^+\pi^-)$ in $\overline{B} \to D^0(\to K^0_S\pi^+\pi^-)\mu^- X$ decays, as determined from the data with (left) downstream and (right) long K^0_S candidates.